

# Pulse phase dependence of emission lines in the X-ray pulsar 4U 1626–67

Aru Beri,<sup>1</sup> Biswajit Paul,<sup>2</sup> Gulab C. Dewangan,<sup>3</sup>

<sup>1</sup>, *Department of Physics, Indian Institute of Technology Ropar, Nangal Road, Rupnagar, Punjab, 140001 India*

<sup>2</sup>, *Raman Research Institute, Sadashivnagar, C. V. Raman Avenue, Bangalore-560 080, India.*

<sup>3</sup>, *Inter University Centre for Astronomy and Astrophysics, Post bag 4, Ganeshkhind, Pune, India.*

26 September 2018

## ABSTRACT

We present results from a pulse phase resolved spectroscopy of the complex emission lines around 1 keV in the unique accretion powered X-ray pulsar 4U 1626–67 using observation made with the *XMM-Newton* in 2003. In this source, the red and blue shifted emission lines and the line widths measured earlier with *Chandra* suggest their accretion disk origin. Another possible signature of lines produced in accretion disk can be a modulation of the line strength with pulse phase. We found the line fluxes to have pulse phase dependence, making 4U 1626–67 only the second pulsar after Her X–1 to show such variability. The O VII line at 0.568 keV from 4U 1626–67 varied by a factor of  $\sim 4$ , stronger than the continuum variability, that support their accretion disk origin. The line flux variability may appear due to variable illumination of the accretion disk by the pulsar or more likely, a warp like structure in the accretion disk. We also discuss some further possible diagnostics of the accretion disk in 4U 1626–67 with pulse phase resolved emission line spectroscopy.

**Key words:** X-ray: Neutron Stars - accretion, accretion disk - pulsars, individual: 4U 1626–67

## 1 INTRODUCTION

4U 1626–67, discovered with the *Uhuru* satellite (Giacconi et al. 1972) is an accreting X-ray pulsar with a pulse period of 7.7 seconds (Rappaport et al. 1977). It is one of the very few

X-ray pulsars in low mass X-ray binary (LMXB) systems. The magnetic field strength of the neutron star is estimated to be of  $B \approx 4 \times 10^{12}$  Gauss (Coburn et al. 2002; Orlandini et al. 1998; Iwakiri et al. 2012) from the cyclotron line features in its X-ray spectrum at around 37 keV. This system with small mass function of  $f < 1.3 \times 10^{-6} M_{\odot}$  has a neutron star that accretes from an extremely low mass companion ( $\leq 0.1 M_{\odot}$ ) (Middleditch et al. 1981; Levine et al. 1988; Chakrabarty 1998). Jain et al. (2008) reported an upper limit of 10 lt-ms for pulse arrival delay using *RXTE* data. The optical light curve shows reprocessed X-ray pulses at 130.38 mHz with multiple sidebands. The sidebands in the power spectrum revealed an orbital period of 42 minute (Middleditch et al. 1981) that was confirmed by Chakrabarty (1998). The short orbital period suggests that the binary system contains a hydrogen depleted companion (Paczynski & Sienkiewicz 1981). The optical counterpart has strong UV excess and high optical pulse fraction (McClintock et al. 1977, 1980). 4U 1626–67 underwent two torque reversals since its discovery. It was initially observed in a spin-up state (Levine et al. 1988; Nagase 1989), this trend reversed in 1990 and the neutron star began to spin down (Wilson et al. 1993; Bildsten et al. 1994, 1997; Prince et al. 1994; Chakrabarty et al. 1997). After the steady spin-down phase of about 18 years, the neutron star again underwent a torque reversal and made a transition to spin-up state in 2008 (Jain, Paul & Dutta 2010; Camero-Arranz et al. 2010). The pulse profiles of this source show a strong correlation with its torque reversals. The pulse profiles during two spin-up eras were quite similar but they were different in the spin-down era (Beri et al. 2014).

The spectrum of 4U 1626–67 has been studied many times using data from different observatories. Observations with *HEAO 1* (Pravdo et al. 1979), *Tenma* (Kii et al. 1986), *ASCA* (Angelini et al. 1995), *Beppo-SAX* (Orlandini et al. 1998), *Chandra*, *XMM-Newton* (Krauss et al. 2007), *RXTE* (Jain, Paul & Dutta 2010) and *Suzaku* (Camero-Arranz et al. 2012; Iwakiri et al. 2012) showed two component spectrum consisting of a blackbody and a power-law. These continuum spectral parameters showed variation during the eras of torque reversals. The blackbody temperature changed from 0.6 keV to 0.3 keV during first transition from spin-up to spin-down phase (Angelini et al. 1995; Vaughan & Kitamoto 1997; Owens, Oosterbroek & Parmar 1997), followed by transition to value of  $\sim (0.5-0.6)$  keV during second phase of spin-up (Jain, Paul & Dutta 2010; Camero-Arranz et al. 2012). During the first spin-up phase the value of powerlaw photon index was 1.5 (Vaughan & Kitamoto 1997). The spectrum became relatively harder during the spin-down phase with the powerlaw

photon index of 0.4-0.6 (Angelini et al. 1995; Vaughan & Kitamoto 1997; Owens, Oosterbroek & Parmar 1997; Orlandini et al. 1998; Yi & Vishniac 1999) and after the second torque reversal, a photon index of 0.8-1.0 was measured (Jain, Paul & Dutta 2010; Camero-Arranz et al. 2012).

The presence of unusually bright Neon (Ne) and Oxygen (O) lines were reported from many spectroscopic observations (Angelini et al. 1995; Owens, Oosterbroek & Parmar 1997; Schulz et al. 2001; Krauss et al. 2007). The equivalent width and intensity of these emission lines were found to be variable (Camero-Arranz et al. 2012). Observations made with *Chandra* revealed a double peaked nature of these line features, indicating their formation in the accretion disc (Schulz et al. 2001). The presence of these emission lines is quite interesting as these are not observed in any other X-ray pulsar. Oxygen emission lines are observed in both UV and optical spectra. However, optical spectrum of this source lacks in Neon emission features (Homer et al. 2002; Werner et al. 2006).

There was a gradual decrease in the X-ray flux in the 0.3-10.0 keV band during 1977-2005 (Krauss et al. 2007), followed by an increase in the flux during the second torque reversal (Camero-Arranz et al. 2010; Jain, Paul & Dutta 2010). Observations made during spin-down period indicated a variations in flux of low energy emission lines within the same phase of torque reversal. The line intensities measured using *ASCA* data (Angelini et al. 1995) were higher compared to that measured using *BeppoSAX* (Owens, Oosterbroek & Parmar 1997), *Chandra* (Schulz et al. 2001; Krauss et al. 2007), *XMM-Newton* (Krauss et al. 2007) and *Suzaku* (Camero-Arranz et al. 2012). The fluxes of these emission lines increased during transition from spin-down to spin-up (Camero-Arranz et al. 2012).

Pulse-Phase resolved spectroscopy is an important tool to probe into the geometry of the emission region. The broadband X-ray continuum of the source shows a phase dependence (Pravdo et al. 1979; Kii et al. 1986). A phase dependence of 37 keV Cyclotron Resonance Scattering Feature (CRSF) was reported using *Suzaku* data by Iwakiri et al. (2012), where they also observed it to be as an emission feature at certain phases.

We present here a pulse phase resolved spectral analysis of 4U 1626-67 using *XMM-Newton* EPIC-pn observation made in 2003 to show the behaviour of the O VII (0.568 keV), O VIII (0.653 keV), Ne IX (0.915 keV), Ne X (1.021 keV) lines in different spin phases. Using *ASCA* data, Angelini et al. (1995) reported that Ne Ly $\alpha$  has no spin-phase dependence. Here we present more detailed analysis of the emission line fluxes in narrow phase bins using

*XMM-Newton* observation which has higher sensitivity than *ASCA*. The paper is organised as follows: The details of the observation and data reduction procedures are mentioned in section 2, section-3 includes timing analysis of the source, followed by the details of the spectroscopy. Finally, the implications of our results are discussed in section 5.

## 2 XMM-NEWTON OBSERVATIONS AND DATA REDUCTION

*XMM-Newton* operates in the energy range of 0.1-15 keV. The instruments on board *XMM-Newton* are European Photon Imaging Camera (EPIC), Reflection Grating Spectrometer (RGS) and Optical Monitor (OM). EPIC consists of two MOS (Turner et al. 2001) and one PN (Strüder et al. 2001) CCD arrays having moderate spectral resolution and a time resolution in the range of micro-seconds to 2.6 seconds depending on the instrument and the mode of observation. High-resolution spectral information ( $E/dE \approx 300$ ) is provided by the Reflection Grating Spectrometer (RGS) (den Herder et al. 2001). Simultaneous optical/UV observations are made with Optical Monitor (OM).

We have used the longest observation (84 ks) of 4U 1626–67 made with *XMM-Newton* on 20 August 2003 (ObsID-0152620101). The EPIC-pn data of this observation were collected in the small window mode and using the medium filter.

*HEASOFT 6.12* and *SAS-12.0.1* were used for the reduction and extraction. For the extraction of the cleaned EPIC-pn events, standard filters were applied. The observation was checked for the particle background using the *SAS* tool *evselect* and background flares were filtered out prior to spectral extraction. The event files were then checked for pile-up, using *SAS* tool *epatplot* and as EPIC-pn has a fast readout time of 5.7 milliseconds for small window mode it was found that there is no problem of pile up in the source spectrum.

For the extraction of the source spectra and lightcurves, circular region of 40 arcsec radius was selected around the source centroid. For the background spectra and light curve extraction, two off-source regions were used with a radius of 40 arcseconds. Spectral extraction was done with  $PATTERN \leq 4$  and  $FLAG=0$ . For reprocessing of the data and generation of the response files updated version of the current calibration files (ccf)<sup>1</sup> was used.

<sup>1</sup> [http://xmm2.esac.esa.int/external/xmm\\_sw\\_cal/calib/ccf.shtml](http://xmm2.esac.esa.int/external/xmm_sw_cal/calib/ccf.shtml)

### 3 PULSE PROFILES

The energy dependent pulse profiles from this observation have already been reported in Krauss et al. (2007). As a prerequisite to the phase resolved spectroscopy reported in the next section, we have repeated the period analysis. We have derived a pulse period of 7.67548 seconds which is consistent with Krauss et al. (2007). However, the energy resolved pulse profiles shown in the left panel of Figure 1 in different energy bands show substantially more fine structures.

Pulse profile of 4U 1626–67 is known to have strong energy dependence (Rappaport et al. 1977; Joss, Avni & Rappaport 1978; Pravdo et al. 1979; Elsner, Ghosh & Lamb 1980; Kii et al. 1986; Levine et al. 1988; Mihara 1995; Angelini et al. 1995; Krauss et al. 2007; Jain et al. 2008; Iwakiri et al. 2012). Angelini et al. (1995); Krauss et al. (2007) and Jain et al. (2008); Jain, Paul & Dutta (2010) also reported pulse profiles similar to Figure 1 during the spin-down phase of the pulsar. These profiles were significantly different from that obtained in two spin-up eras (Beri et al. 2014).

## 4 SPECTROSCOPY

### 4.1 Pulse Phase averaged Spectroscopy

Pulse-phase averaged spectral analysis was performed using the mean spectrum extracted from the EPIC-pn data, which was then grouped using ftool *grppha* with minimum 500 counts/bin. The spectral fitting was done using *Xspec Version: 12.8.0* (Arnaud 1996). The energy band chosen for fit was 0.3–10.0 keV.

The continuum of the phase averaged spectrum is well described by a soft thermal component and a power law (Pravdo et al. 1979; Kii et al. 1986; Angelini et al. 1995; Owens, Oosterbroek & Parmar 1997; Orlandini et al. 1998; Schulz et al. 2001; Krauss et al. 2007; Jain, Paul & Dutta 2010; Camero-Arranz et al. 2012; Iwakiri et al. 2012). The two components cross over at 0.8 keV. We used *bbodyrad* model for fitting the soft part of the spectrum.

Using only the continuum model shows significant excess in the form of emission line features around 0.5 keV and 1.0 keV (see Figure 2). The *RGS* data from the same *XMM-Newton* observation was used by Krauss et al. (2007), where they found four emission lines at 0.568, 0.653, 0.915, 1.02 keV. All the four lines were found to be narrow ( $\sigma \sim 1\text{eV}$ ). Following those results we added four Gaussian lines with energies fixed at 0.568 (O VII

**Table 1.** Best-fitting parameters of Phase averaged spectrum of 4U1626-67.

Parameter	Model Values
$N_H$ ( $10^{22}$ atoms $\text{cm}^{-2}$ )	$0.102 \pm 0.001$
PowIndex ( $\Gamma$ )	$0.793 \pm 0.003$
$N_{PL}^a$	$0.00656 \pm .00004$
BBody (kT) keV	$0.229 \pm 0.001$
$N_{BB}^b$	$441 \pm 18$
LineFlux <sup>c</sup>	
O VII (0.568 keV)	$6.4 \pm 0.1$
O VIII (0.653 keV)	$3.7 \pm 0.1$
Ne IX (0.915 keV)	$1.36 \pm 0.09$
Ne X (1.02 keV)	$1.88 \pm 0.07$

**Notes:** Errors quoted are for the 68 % confidence range.

a  $\rightarrow$  Powerlaw normalisation ( $N_{PL}$ ) is in units of photons  $\text{cm}^{-2} \text{s}^{-1} \text{keV}^{-1}$  at 1 keV

b  $\rightarrow$  Blackbody normalisation ( $N_{BB}$ ) is in units of photons  $\text{cm}^{-2} \text{s}^{-1} \text{keV}^{-1}$

c  $\rightarrow$  Gaussian normalisation is in units of  $10^{-4}$  photons  $\text{cm}^{-2} \text{s}^{-1}$

$He_\alpha$ ), 0.653 (O VIII  $Ly_\alpha$ ), 0.915 (Ne IX  $He_\alpha$ ) and 1.02 keV (Ne X  $Ly_\alpha$ ) to the continuum model, with their line widths fixed to  $\sigma=1$  eV. On adding these lines an improved good fit was obtained with reduced  $\chi^2$  ( $\chi_\nu^2$ ) of 1.175 for 1224 dof. The best fit parameters are given in Table-1. These fit parameters are in good agreement with the values reported by Krauss et al. (2007) using *RGS* data from the same observation.

## 4.2 Phase-Resolved Spectroscopy

The energy dependence of the pulse profiles in Figure 1, suggests a clear dependence of the energy spectrum on the spin phase. A strong phase dependence of the continuum of 4U 1626–67 has been reported by Pravdo et al. (1979), Kii et al. (1986), Coburn et al. (2000) and Iwakiri et al. (2012) using the phase resolved spectra acquired by *HEAO-1*, *Tenma*, *RXTE* and *Suzaku* respectively.

In order to investigate the correlation between the features observed in the pulse profiles with Neon and Oxygen emission lines in the spectrum of 4U 1626–67 we performed a pulse-phase resolved spectroscopy. For the phase resolved spectral analysis, the spectra were extracted with a phase bin of 0.05, using the ‘phase’ filter of *ftools*<sup>1</sup> task XSELECT. We used the same background spectrum and response files as were used for the phase-averaged spectrum. X-ray spectra in different phases were grouped using *ftools* task GRPPHA with minimum 250 counts per bin. For fitting the phase-resolved spectra we followed exactly the same technique as we opted for the phase-averaged spectrum.

<sup>1</sup> <http://heasarc.gsfc.nasa.gov/ftools/>

The continuum parameters (Figure 3) show variation with the pulse phase. The equivalent hydrogen column density ( $N_H$ ) showed significantly higher value compared to the average value in the phase range 0.7-1.15 with some fluctuation. Temperature of blackbody varied within the range of  $\sim 0.16$ -0.30 keV showing lower value around phase 0.7-1.15. The normalisation of blackbody also exhibits a behaviour that is anticorrelated with its temperature profile. However, we note that these spectral parameters can have degeneracy between them and the rapid fluctuations of these parameter as seen in Figure 3 does indicate the presence of significant degeneracy. We therefore do not comment further on this. The power-law index however is determined from a broader energy range and shows lesser bin to bin fluctuation. We find a pulse phase dependence of the power-law index with spectrum being hardest near the pulse peak and it being soft near the dip of the pulse profile.

Right panel in Figure 1 shows the behaviour of total flux, blackbody flux, power law flux, Ne and O line intensities as function of the pulse phase. The total and power law flux show a sharp dip at around phase 1.0 along with two shallow dips near phase 0.3 and 0.7. This trend is quite similar to that of its pulse profile. Blackbody flux also shows some structures in its profile with a dip between 0.2-0.3 phase. The behaviour of line fluxes shown in Figure 1 is compared to the features in its pulse profile.

1.) The O VII (0.568 keV) emission line shows strong variability by more than a factor of 4. This line is in maximum between the phase 0.0-0.15 and then decreases reaching a minimum intensity at around phase of 0.3. In the rest of the pulse phase also it shows some variation. It is interesting to note that peak intensity of this line is coincident with dip in the pulse profile.

2.) The O VIII (0.653 keV) shows some variation with spin phase but without any clear structures in it.

3.) Ne IX (0.915 keV) shows some variation with spin phase with a possible correlation with the pulse profile in 0.8-1.2 keV energy band.

4.) The Ne X (1.021 keV) line is consistent with no pulse phase dependence.

The equivalent width (EW) of these emission lines are shown in Figure 4. The EW of 0.568 keV line also shows a maximum around phase 0.0-0.15 with a subsequent decreasing trend till phase 0.3. Some variation in the EW of this line is seen throughout the pulse

phase. The EW of 0.615 keV line also show variation with phase. A dip in the EW profile of 0.915 keV emission line is coincident with the main dip observed in the pulse profile as well as its flux profile. However, the EW of 1.02 keV emission line is almost constant throughout its pulse phase.

To evaluate the statistical significance of variation of the O VII (0.568 KeV) line with spin phase, we fixed the norm of the line in the phase resolved spectra with the value obtained from the phase-averaged spectrum. Fixing the line intensity to its phase averaged value resulted into an increase in the chi-squared ( $\chi^2$ ) by upto 36 for 230 degrees of freedom (dof). In 5 of the 20 phase bins, the chance probability for the increase in  $\chi^2$  is determined by F-test to be less than  $10^{-4}$  and in one of the bins it is as low as  $5 \times 10^{-8}$ , which clearly demonstrates the variation of the O VII emission line.

A constant fitted to the flux (Figure 1) and equivalent width (Figure 4) of the O VII line returned  $\chi^2$  values of 46 and 32 respectively for the 20 phase bins, which is another measure of the significance of the flux variability.

To further inspect the significance of the line intensity variation, we have plotted the fraction of the number of phase bins for which the line flux differs from the average value by more than  $N\sigma$  as a function of  $N$ . The same is compared with what is expected without any intrinsic variability of the line (Figure 5). For any phase bin there is only 0.27 % chance probability for a  $3\sigma$  deviation while in three of the 20 phase bins in Figure 5 the line flux deviates from the pulse averaged value by more than  $3\sigma$  showing that the variability is statistically significant.

We have also made a direct comparison of the spectra extracted in the pulse phase ranges 0.0-0.15 and 0.15-0.4. At these phases, flux of this line shows maximum variation. In Figure 6, we have shown the best fitted spectra along with the model components in top panels for these two phase ranges. In the middle panels of the respective figures, we have shown the residuals obtained for the best fit and in the bottom panels the residuals are shown after setting the model line fluxes to zero. The residuals in the bottom panels clearly show the flux difference for the 0.568 keV line.

To further investigate significance of the detected variation of the O VII line flux we simulated 10,000 spectra using the model parameters of the phase averaged spectrum, with an exposure time typical of a phase resolved spectra (2921 seconds). In each simulation, all the spectral parameters were taken to be same as their phase averaged values. Thereafter,



these simulated spectra were fitted using the same model allowing all but the energy and widths of the four lines to vary. A constant fitted to the flux of O VII line returned a  $\chi^2$  value of 8586 for 10,000 data points. We found that standard deviation of the O VII line flux variation in the simulated spectra was merely 15.2%, and 90% of the simulation results had flux within -36% and +40% of the average value. Thus the variation of line flux found in the simulated spectra is quite low compared to upto a factor of 4 variation observed in the O VII line flux, indicating that degeneracy between the spectral parameters did not result into values of the narrow line fluxes.

Moreover, we have also performed similar analysis with different trial pulse periods of 6, 7 and 8 seconds. The phase resolved spectra created using these trial periods were fitted using the same model. We did not find any significant variation of O VII line flux at these arbitrary trial periods. The constant fitted to the flux of O VII line flux shown in Figure 7 returned  $\chi^2$  values of 16, 16 and 20 for 19 dof with the periods 6, 7 and 8 seconds respectively, compared to 46 for *XMM-Newton* data. This probe further strengthens our result of variation of O VII line flux accross the pulse phase.

We also created pulse profiles in very narrow energy bands (of range of about 0.1 keV) to compare the shape of the profiles near 0.568 keV with that of the higher and lower energy continuum. However, because of the fact that the equivalent width (EW) of these emission lines is quite low (10-30 eV) in comparison to the energy resolution of about 100 eV and these line energies contribute to a small fraction of emission even for a band width of 100 eV, the difference between the pulse profiles was not very prominent, though we could observe some differences in the sharpness of the dips in the profiles. This was also consistent with our results obtained from pulse phase resolved spectroscopy.

## 5 DISCUSSIONS AND CONCLUSIONS

In the present work, we have performed a detailed pulse-phase resolved spectroscopy of the unique high magnetic field LMXB pulsar 4U 1626–67 using data from EPIC-pn onboard *XMM-Newton* observatory to investigate the flux variation of complex emission lines arising from the highly ionised species of Ne and O (Angelini et al. 1995; Owens, Oosterbroek & Parmar 1997; Krauss et al. 2007) in order to investigate the origin of this unusual complex of emission

lines. *Chandra*-HETG observations of 4U 1626-67 made in 2001 revealed a double peaked nature of these lines (Schulz et al. 2001) interpreted as Doppler pairs of broadened lines of hydrogenic and He like Ne and O. The Doppler velocity corresponding to the widths of these lines is of the same order as Keplerian velocities in the accretion disks. Schulz et al. (2001) have also mentioned the less likely possibility of Doppler shifted lines originating in a bipolar disk outflow. In the case of an accretion disk origin, lines of different elements and ionisation states will be produced in different annular regions of the accretion disk, at the corresponding values of the ionisation parameter.

Emission lines, especially the iron fluorescence line at 6.4 keV is ubiquitous among the X-ray pulsars and has various origins like the accretion disk, strong stellar wind of the high mass companion, accretion stream from the companion star, outflowing disk of the Be-star companions etc. The line flux is usually found to be variable, both with the continuum flux and with the absorption column density (Inoue 1985; Makishima 1986; Kotani et al. 1999; Naik & Paul 2003; Fürst et al. 2011). However, in the accretion powered pulsars, the line flux is often found to have no pulse phase dependence (Paul et al. 2002; Lei et al. 2009; Wilkinson et al. 2011; Suchy et al. 2012). An exception is a strong pulse phase dependence of the 6.4 keV line seen in Hercules X-1 (Vasco et al. 2013) in which the line flux is found to be minimum near the pulse peak and there is a remarkable similarity between the pulse phase dependence of the iron line flux and the power-law photon index.

Pulse phase resolved spectroscopy of 4U 1626-67 carried out in 20 bins show a strong flux variation of O VII (0.568 keV) line with pulse phase. We have also shown a comparison of spectrum in two phase ranges (0.0-0.15) and (0.15-0.4) where the flux of this line shows maximum difference. However, we would like to add a caveat that if a part of the line of sight absorption column is local to the source with a pulse phase dependent ionisation state of the material, the same can introduce some unforeseen artifacts in the phase resolved measurements of the line parameters. Unfortunately, it is not possible to investigate this with a pulse phase resolved spectroscopy of the *RGS* data. The two lines O VIII (0.653 keV) and Ne IX (0.915 keV) show weak variation with phase while the Ne X (1.021 keV) line is consistent with being non-varying.

In 4U 1626-67, we found the O VII line flux to vary by factor of about four (maxi-

mum/minimum; Figure 1: 4<sup>th</sup> panel on the right column), significantly larger compared to the relative variation of total flux ( Figure 1: top panel on right column). This indicates that the line flux variation is unlikely to be due to varying illumination of flat accretion disk. The dimension of the accretion disk in 4U 1626–67, which has an orbital period of about 40 minutes is about 0.5 lt-sec which is also smaller than the variability time scale observed for the line flux, about 2 seconds. Thus, one possibility of the observed line flux variation could be warps in the accretion disk. Milli-Hertz QPOs in the UV and optical lightcurves of 4U 1626–67 have been interpreted as signature of warps in its accretion disk (Chakrabarty et al. 2001). In the presence of warps, the visibility of the X-ray illuminated part of the accretion disk can have significant variation with pulse phase. If any of the emission lines is produced at the same radius as the warp, it may result into a pulse phase dependent line flux. A very low upper limit of mass function obtained from pulse arrival time delay (Levine et al. 1988; Jain et al. 2008) indicates a very small mass of the companion star or a large angle of the orbital plane, or a combination of both. While much of the accretion disk is likely to be in the orbital plane, the line production region (inner accretion disk) probably has warped structure and has a different inclination, which is also borne out from the mHz QPOs (Chakrabarty et al. 2001).

Though the results presented here are indicative of an accretion disk with a warp around a distance at which the O VII emission line is produced, it is also possible to produce a large flux variation of one emission line if the accretion disk sees a very different pulse profile compared to the observer and if the lines produced have different escape probability. Since, only O VII emission line showed strong variation accross the pulse phase, it may be possible one of the component of triplet O VII emission line may have higher escape probability.

The X-ray timing characteristics, like the pulse profile, the QPO’s etc of 4U 1626–67 are known to be different in the spin-down phase compared to spin-up phase (Jain, Paul & Dutta 2010; Beri et al. 2014) which may also be caused by a difference in the inner accretion flow from a warped accretion disk in the spin-down phase. If this scenario is true, the Doppler characteristics of the O and Ne lines are expected to be different in the current spin-up phase of 4U 1626–67. We also note that Her X-1 is known to have a warped accretion disk, but the pulse phase dependence of the iron line flux in Her X-1 is almost identical in the different superorbital phases (Vasco et al. 2013) which is caused by precession of the warped

structure. Thus the variation of the line flux in the two sources 4U 1626–67 and Her X-1 have different origin and the latter is explained to be due to reprocessing of continuum X-ray in the accretion column with hollow cone geometry.

## 6 SUMMARY

We have found the O VII emission line in the spectrum of the accretion powered pulsar 4U 1626–67 to vary with pulse phase, the only pulsar after Her X-1 to show a pulse dependent emission line flux. The flux variation is by a factor of up to 4, much larger than the pulse fraction, indicating the presence of warp in the accretion disk at the same radius at which this line is produced by reprocessing of the X-rays emitted from the neutron star. This is also the first X-ray spectroscopic evidence of an accretion disk warp in an X-ray binary.

## ACKNOWLEDGMENTS

A.B would like to thank all the members of the 2nd X-ray Astronomy workshop, held in IUCAA, Pune, India, 2013 and also acknowledges IIT ropar for financial assistance and Raman Research Institute (RRI) for providing local hospitality. The research has made use of data obtained from High Energy Astrophysics Science Archive Research Center (HEASARC), provided by NASA Goddard Space Flight Center. We thank an anonymous referee for very constructive and useful comments, which improved the paper.

## REFERENCES

- Angelini L., White N. E., Nagase F., Kallman T. R., Yoshida A., Takeshima T., Becker C., Paerels F., 1995, *ApJ*, 449, L41
- Arnaud K. A., 1996, in *Astronomical Society of the Pacific Conference Series*, Vol. 101, *Astronomical Data Analysis Software and Systems V*, Jacoby G. H., Barnes J., eds., p. 17
- Beri A., Jain C., Paul B., Raichur H., 2014, *MNRAS*, 439, 1940
- Bildsten L., Chakrabarty D., Chiu J., Finger M. H., Grunsfeld J. M., Koh T., Prince T. A., Wilson R., 1994, in *American Institute of Physics Conference Series*, Vol. 304, *American Institute of Physics Conference Series*, Fichtel C. E., Gehrels N., Norris J. P., eds., pp. 294–298
- Bildsten L. et al., 1997, *ApJS*, 113, 367

- Camero-Arranz A., Finger M. H., Ikhsanov N. R., Wilson-Hodge C. A., Beklen E., 2010, *ApJ*, 708, 1500
- Camero-Arranz A., Pottschmidt K., Finger M. H., Ikhsanov N. R., Wilson-Hodge C. A., Marcu D. M., 2012, *A&A*, 546, A40
- Chakrabarty D., 1998, *ApJ*, 492, 342
- Chakrabarty D. et al., 1997, *ApJ*, 474, 414
- Chakrabarty D., Homer L., Charles P. A., O’Donoghue D., 2001, *ApJ*, 562, 985
- Coburn W., Heindl W. A., Gruber D. E., Rothschild R. E., Staubert R., Wilms J., Kreykenbohm I., 2000, in *Bulletin of the American Astronomical Society*, Vol. 32, AAS/High Energy Astrophysics Division #5, p. 1213
- Coburn W., Heindl W. A., Rothschild R. E., Gruber D. E., Kreykenbohm I., Wilms J., Kretschmar P., Staubert R., 2002, *ApJ*, 580, 394
- den Herder J. W. et al., 2001, *A&A*, 365, L7
- Elsner R. F., Ghosh P., Lamb F. K., 1980, *ApJ*, 241, L155
- Fürst F. et al., 2011, *A&A*, 535, A9
- Giacconi R., Murray S., Gursky H., Kellogg E., Schreier E., Tananbaum H., 1972, *ApJ*, 178, 281
- Homer L., Anderson S. F., Wachter S., Margon B., 2002, *AJ*, 124, 3348
- Inoue H., 1985, *Space Sci. Rev.*, 40, 317
- Iwakiri W. B. et al., 2012, *ApJ*, 751, 35
- Jain C., Paul B., Dutta A., 2010, *MNRAS*, 403, 920
- Jain C., Paul B., Joshi K., Dutta A., Raichur H., 2008, *Journal of Astrophysics and Astronomy*, 28, 175
- Joss P. C., Avni Y., Rappaport S., 1978, *ApJ*, 221, 645
- Kii T., Hayakawa S., Nagase F., Ikegami T., Kawai N., 1986, *PASJ*, 38, 751
- Kotani T., Dotani T., Nagase F., Greenhill J. G., Pravdo S. H., Angelini L., 1999, *ApJ*, 510, 369
- Krauss M. I., Schulz N. S., Chakrabarty D., Juett A. M., Cottam J., 2007, *ApJ*, 660, 605
- Lei Y.-J., Chen W., Qu J.-L., Song L.-M., Zhang S., Lu Y., Zhang H.-T., Li T.-P., 2009, *ApJ*, 707, 1016
- Levine A., Ma C. P., McClintock J., Rappaport S., van der Klis M., Verbunt F., 1988, *ApJ*, 327, 732
- Makishima K., 1986, in *Lecture Notes in Physics*, Berlin Springer Verlag, Vol. 266, The

- Physics of Accretion onto Compact Objects, Mason K. O., Watson M. G., White N. E., eds., p. 249
- McClintock J. E., Bradt H. V., Doxsey R. E., Jernigan J. G., Canizares C. R., Hiltner W. A., 1977, *Nature*, 270, 320
- McClintock J. E., Li F. K., Canizares C. R., Grindlay J. E., 1980, *ApJ*, 235, L81
- Middleditch J., Mason K. O., Nelson J. E., White N. E., 1981, *ApJ*, 244, 1001
- Mihara T., 1995, PhD thesis, , Dept. of Physics, Univ. of Tokyo (M95), (1995)
- Nagase F., 1989, *PASJ*, 41, 1
- Naik S., Paul B., 2003, *A&A*, 401, 265
- Orlandini M. et al., 1998, *ApJ*, 500, L163
- Owens A., Oosterbroek T., Parmar A. N., 1997, *A&A*, 324, L9
- Paczynski B., Sienkiewicz R., 1981, *ApJ*, 248, L27
- Paul B., Dewangan G. C., Sako M., Kahn S. M., Paerels F., Liedahl D., Wojdowski P., Nagase F., 2002, in 8th Asian-Pacific Regional Meeting, Volume II, Ikeuchi S., Hearnshaw J., Hanawa T., eds., pp. 355–356
- Pravdo S. H. et al., 1979, *ApJ*, 231, 912
- Prince T. A., Bildsten L., Chakrabarty D., kinsomnson R. B., Finger M. H., 1994, in American Institute of Physics Conference Series, Vol. 308, The Evolution of X-ray Binaries, Holt S., Day C. S., eds., p. 235
- Rappaport S., Markert T., Li F. K., Clark G. W., Jernigan J. G., McClintock J. E., 1977, *ApJ*, 217, L29
- Schulz N. S., Chakrabarty D., Marshall H. L., Canizares C. R., Lee J. C., Houck J., 2001, *ApJ*, 563, 941
- Strüder L. et al., 2001, *A&A*, 365, L18
- Suchy S., Fürst F., Pottschmidt K., Caballero I., Kreykenbohm I., Wilms J., Markowitz A., Rothschild R. E., 2012, *ApJ*, 745, 124
- Turner M. J. L. et al., 2001, *A&A*, 365, L27
- Vasco D., Staubert R., Klochkov D., Santangelo A., Shakura N., Postnov K., 2013, *A&A*, 550, A111
- Vaughan B. A., Kitamoto S., 1997, arXiv:astro-ph/9707105
- Werner K., Nagel T., Rauch T., Hammer N. J., Dreizler S., 2006, *A&A*, 450, 725
- Wilkinson T., Patruno A., Watts A., Uttley P., 2011, *MNRAS*, 410, 1513
- Wilson R. B., Fishman G. J., Finger M. H., Pendleton G. N., Prince T. A., Chakrabarty

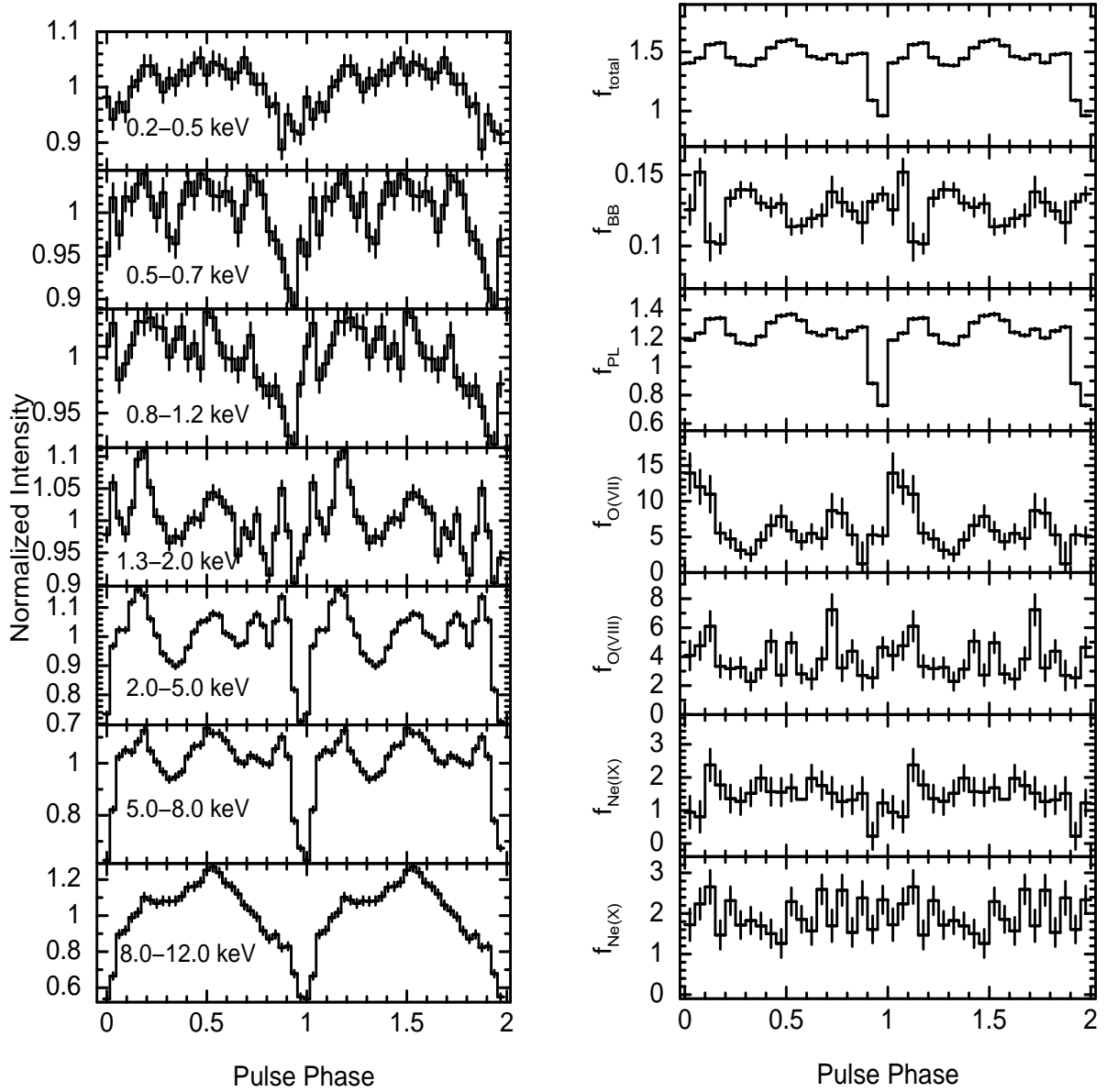


**Figure 1.** The left-hand panels show the energy resolved pulse profiles created using EPIC-pn data and binned into 32 phasebins. The right panel shows the variation of flux ( $f$ ) of continuum and the low energy emission lines near 1 keV with the pulse phase. The units of all continuum fluxes ( $f_{\text{total}}$ ,  $f_{\text{BB}}$ ,  $f_{\text{PL}}$ ) are in  $10^{-10} \text{ ergs cm}^{-2} \text{ sec}^{-1}$ , while the line fluxes are measured in units of  $10^{-4} \text{ photons cm}^{-2} \text{ sec}^{-1}$ . All the errors were estimated with  $1\sigma$  confidence.

D., 1993, in American Institute of Physics Conference Series, Vol. 280, American Institute of Physics Conference Series, Friedlander M., Gehrels N., Macomb D. J., eds., pp. 291–302  
 Yi I., Vishniac E. T., 1999, ApJ, 516, L87

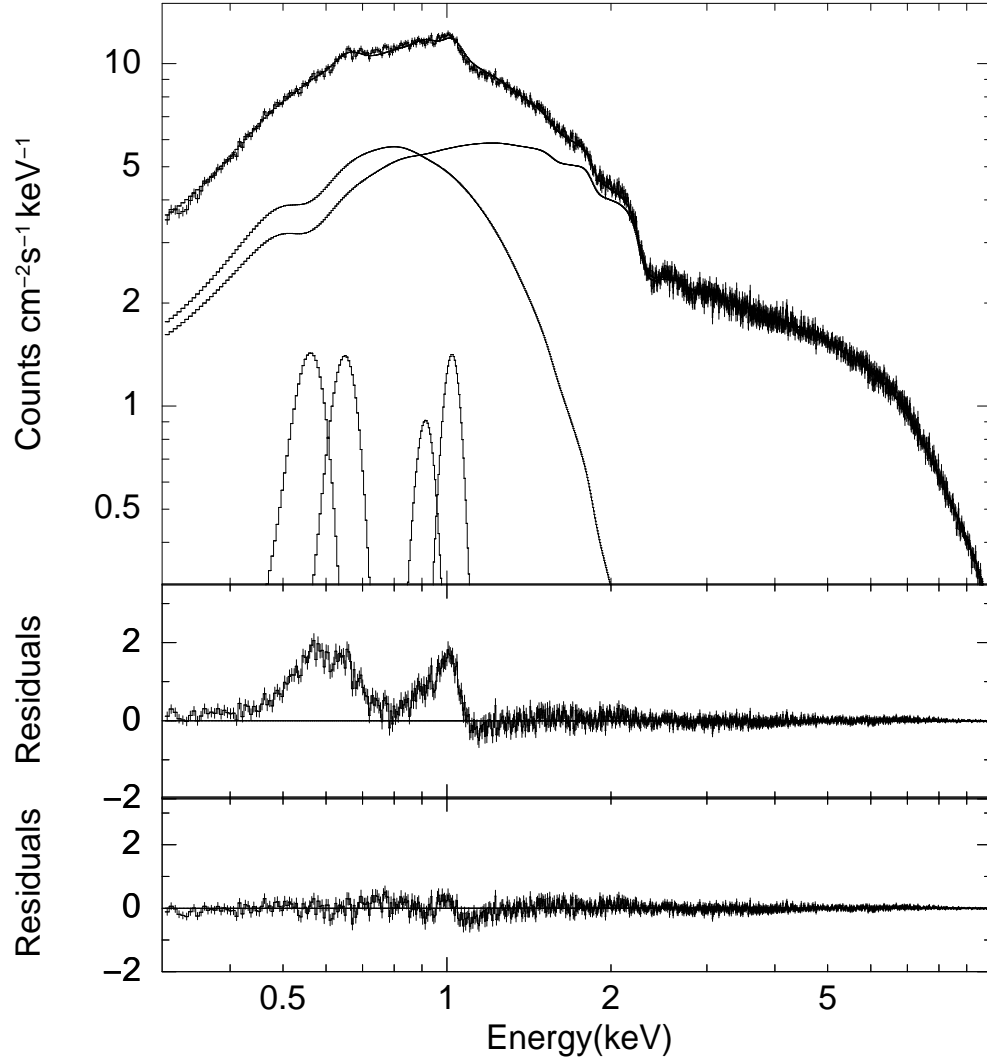


**Figure 2.** Data and folded model of 4U 1626–67 from *XMM-Newton* EPIC-pn. Upper panel shows the phase averaged spectrum. The thick line is the best fit model obtained by fitting the continuum (consisting bbody and power-law). Middle panel show the residuals ( $\text{Counts cm}^{-2}\text{s}^{-1}\text{keV}^{-1}$ ) obtained, using only continuum models and the lower panel are the residuals ( $\text{Counts cm}^{-2}\text{s}^{-1}\text{keV}^{-1}$ ) after fitting gaussians at 0.568 keV, 0.653 keV, 0.915 keV and 1.02 keV energies along with continuum models.



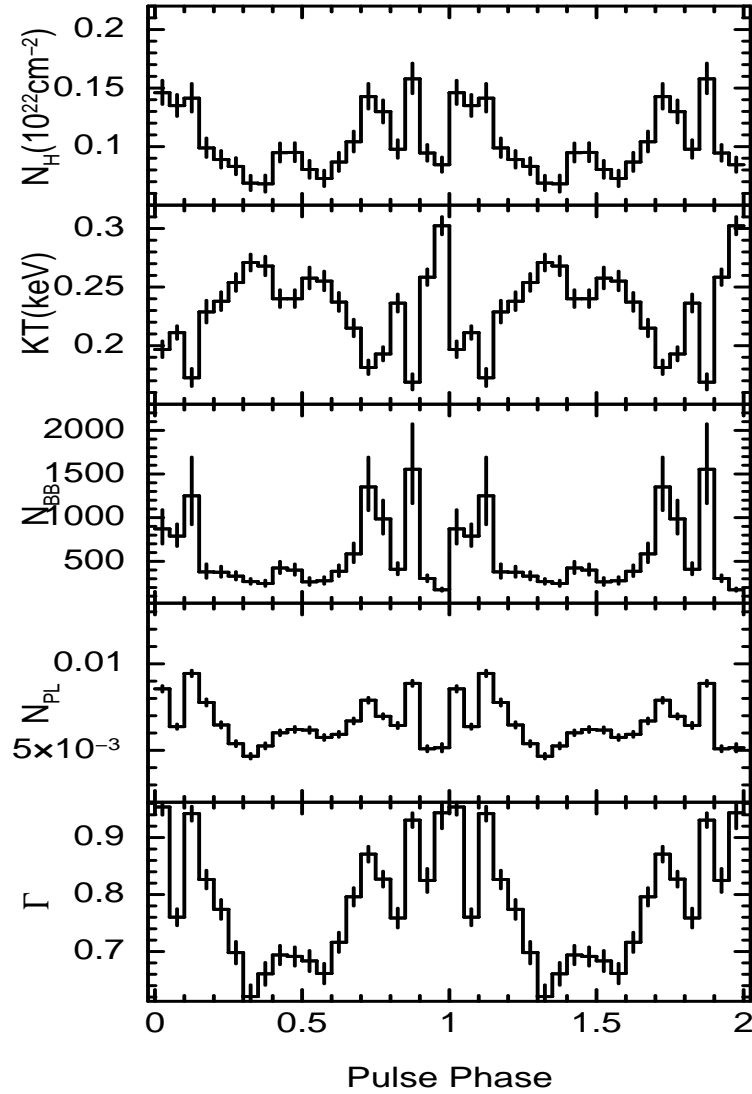


**Figure 3.** Variation of spectral parameters of continuum across the pulse phase for 4U 1626–67. The units of  $N_H$  (equivalent hydrogen column density) is  $10^{22} \text{atoms cm}^{-2}$ . Power-law ( $N_{PL}$ ) and blackbody normalisations ( $N_{BB}$ ) is in units of  $\text{photons keV}^{-1} \text{cm}^{-2} \text{s}^{-1}$ . All the values are in  $1\sigma$  confidence.

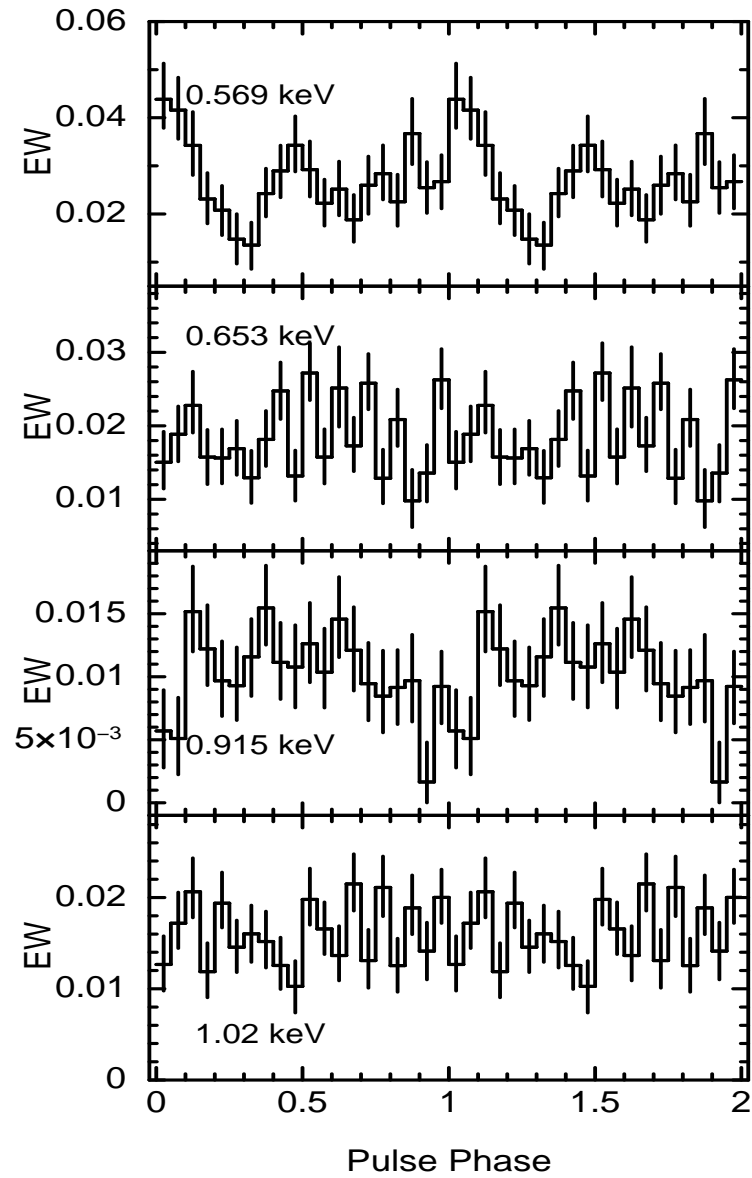


**Figure 4.** Equivalent widths (EW) of Ne and O lines as the function of phase for 4U1626-67. EW is measured in units of keV. The errors were estimated with  $1\sigma$  confidence.

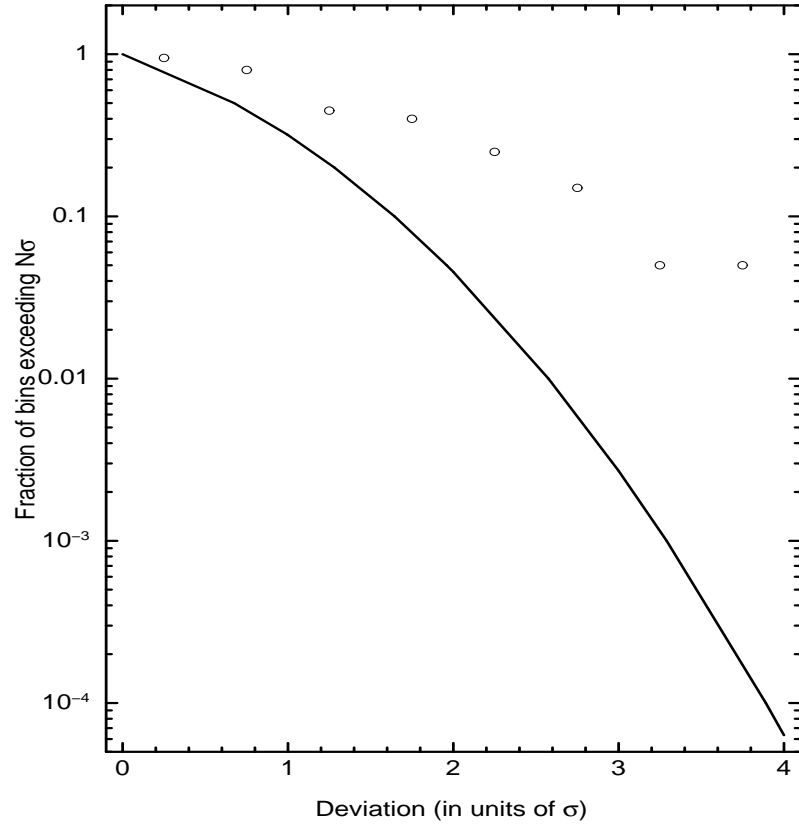


**Figure 5.** The deviation of the flux of the O VII line with pulse phase with respect to the average flux is shown here. The fraction of the number of bins that deviates by more than  $N\sigma$  is plotted as a function of  $N$ . The same for purely statistical variation is shown with a line. The y-axis is in log scale.

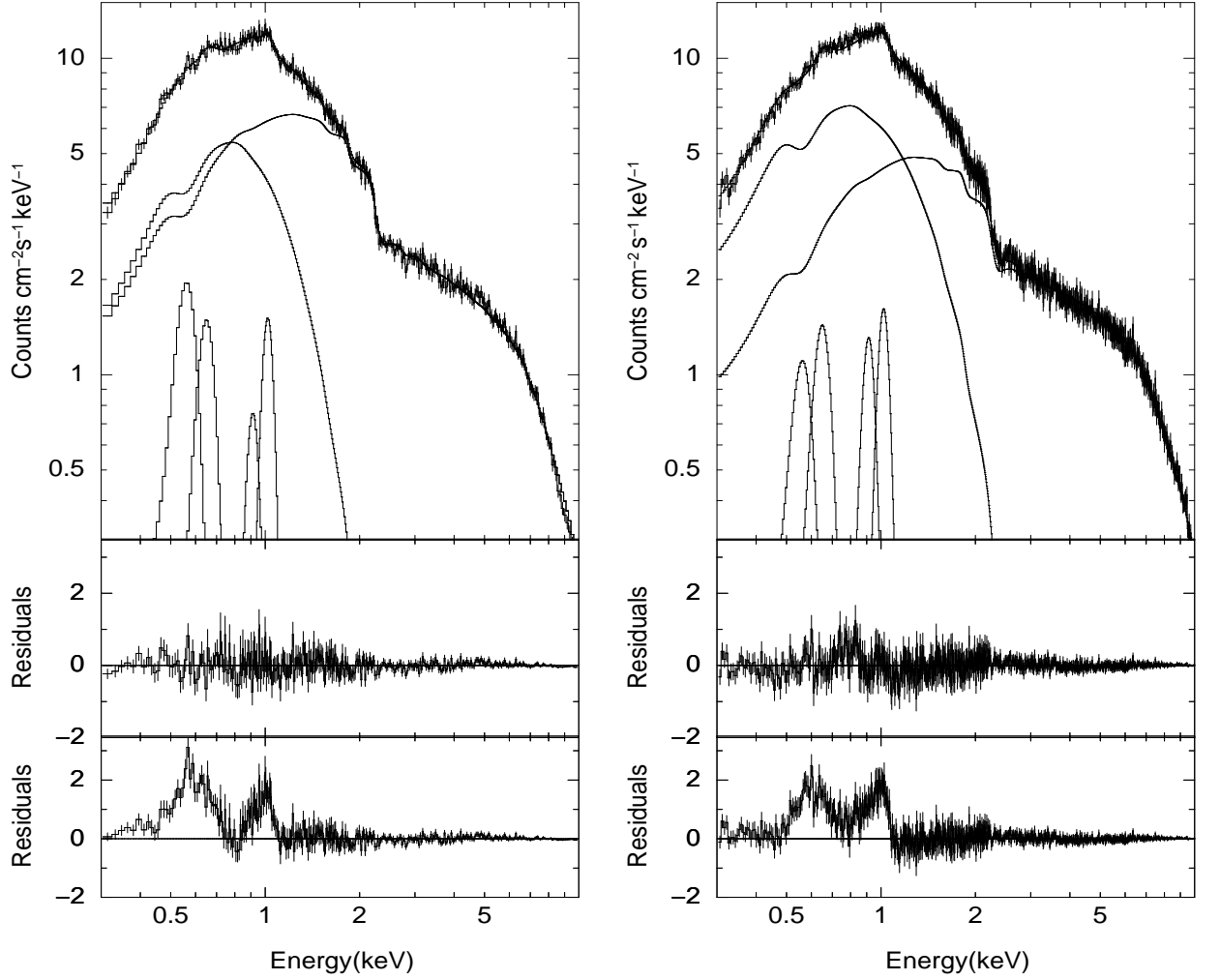


**Figure 6.** In the left, panel-1 shows data and the best fit models of the spectrum extracted in (0.0-0.15) phase range, the middle panel shows the residuals ( $\text{Counts cm}^{-2}\text{sec}^{-1}\text{keV}^{-1}$ ) for the best fit and the bottom panel shows the residuals after setting line fluxes to zero. Similarly, in the right, the top panel shows data and the best fit models of the spectrum extracted in (0.15-0.4) phase range, second panels contains the residuals obtained with best fit while the bottom panel has residuals with normalisations set to zero of line fluxes. Note the difference of the flux of the first emission line around 0.569 keV.

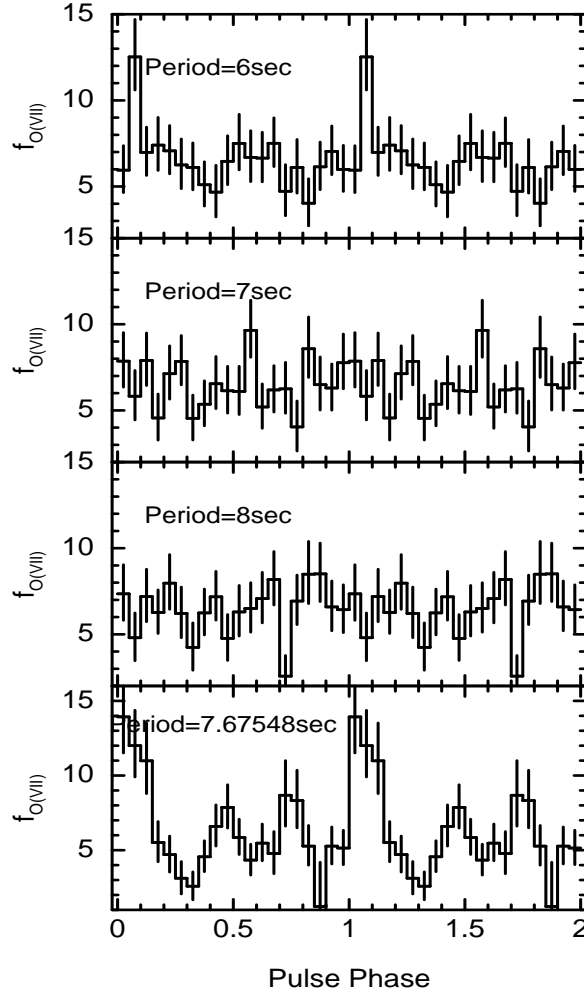


Figure 7. The variation of flux ( $f$ ) of O VII emission line across the pulse phase using different trial periods in comparison to the true period=7.67548 seconds. The line flux is measured in units of  $10^{-4} \text{photons cm}^{-2} \text{sec}^{-1}$ . All the errors were estimated with  $1\sigma$  confidence.